

## 1 Abstract

Hysteresis characteristics of the general Spin- $S$  ( $S > 1$ ) Blume-Capel model have been studied within the effective field approximation. Particular emphasis has been paid on the large negative valued crystal field region and it has been demonstrated for this region that, Spin- $S$  Blume-Capel model has  $2S$  windowed hysteresis loop in low temperatures. Some interesting results have been obtained such as nested characteristics of the hysteresis loops of successive spin- $S$  Blume-Capel model. Effect of the rising crystal field and temperature on these hysteresis behaviors have been investigated in detail and physical mechanisms have been given.

## 2 Introduction

Higher spin Ising model ( $S > 1$ ) is very important for understanding of the real magnetic materials. Although  $S = 1/2$  problems are the most widely studied in the literature on the theoretical side, it is a well known fact that  $S = 1/2$  systems are highly idealized systems. For instance none of the known ferromagnetic/antiferromagnetic atom in the periodic table has  $1/2$ . When the atoms brought together in a solid, different spin values emerge due to the overlapping of the atomic orbitals of the constituent atoms. Indeed, there are numerous molecules that have very high spins in the ground state, for instance  $S = 6$  [1],  $S = 8$ ,  $S = 10$  [2]. Besides, the most of the magnetic materials are represented by higher spin systems. For instance bimetallic Prussian blue analogs  $CsNi^{II}[Cr^{III}(CN)_6] \cdot (H_2O)$  can be represented by  $S = 3/2$ ,  $S = 1$ ,  $S = 2$  atoms on the lattice [3]. Although it is very important to investigate higher spin systems, there is a downward trend with the rising spin value in the theoretical literature. This is due to the fact that, rising computational time for simulations and rising mathematical difficulties for approximation schemes for greater spin values.

Ising model including the crystal field or the single-ion anisotropy was introduced as a  $S = 1$  Blume - Capel (BC) model [4, 5]. Later on, it was generalized to the higher spin problems and solved within the mean field approximation (MFA) [6]. Some variants of the model exist such as spin- $S$  model with biquadratic exchange interaction and it was solved within the cluster variation method [7, 8]. Also, transverse Ising model with higher spin has been solved within the effective field theory (EFT) [9–11]. Quenched disorder effects such as site dilution has been also investigated for spin- $S$  BC model with EFT [12, 13] and random crystal field problem within the pair approximation [14]. Some other techniques such as Monte Carlo (MC) simulation exist for the higher spin BC model [15]. This short literature was for the general spin- $S$  models. If we look at the specific spin valued BC model, we see downward trend with rising spin values.

$S = 3/2$  BC model have been introduced earlier to explain the phase transitions in  $DyVO_4$  [16, 17] and tricritical properties of the ternary fluid mixtures [18]. This model has been solved by various methods such as EFT [19–22], two spin cluster approximation [23], thermodynamically self consistent theory [24], finite size scaling [25], MC and density matrix renormalization group technique [26], renormalization group technique (RG) [27]. Antiferromagnetic BC model has already been worked within the MFA [28], cluster variation method [29], transfer matrix technique [30], transfer-matrix finite-size-scaling calculations and MC [31]. Besides,  $S = 3/2$  BC model with bilinear and biquadratic interactions has been investigated [32–34]. If we look at different geometries we can see that  $S = 3/2$  model within different geometries have also been worked such as Bethe lattice [35–37], multilayer [38, 39], cylindrical Ising nanotube [40], hexagonal Ising nanowire [41] and semi infinite geometry [42]. Some generalizations of the  $S = 3/2$  Ising model have already been constructed and solved.  $S = 3/2$  Ising model with transverse field [43–51], and transverse

---

<sup>1</sup>umit.akinci@deu.edu.tr

crystal field [52,53] are among them. Quenched disorder effects, which is another important topic is widely worked out for the  $S - 3/2$  Ising model. Effect of the discrete random longitudinal field distribution (bimodal distribution) [54–58] and random crystal field distribution [59–61], random bond distribution [62–64], bond dilution [65], site dilution [66,67] problems have been worked out. Note that, EFT has been used in most of these quenched disorder works.

$S - 2$  Ising model is also important due to the experimental realizations. For instance the spin values of  $FeII$  ions are 2 and it is experimentally found that these ions have anisotropy [68]. Also for the disordered  $Fe_{(1-q)}Al_q$  alloys, it has been demonstrated that the effective spin value of iron is 2 and 5/2 for Fe 2+ and Fe 3+ ions, respectively [69]. Fe-Al alloys has been modeled and solved by EFT [70]. As in  $S - 3/2$  models, EFT is dominant method for the aim of determining critical and thermodynamical properties of the  $S - 2$  Ising model. EFT is successfully applied to the  $S - 2$  Ising model with transverse field [71–74], transverse crystal field [75], discrete distributed random field [76,77], random crystal field [78], site dilution problems [79,80] and the model with biaxial crystal field [81]. MFA has also been applied to the  $S - 2$  Ising model with transverse field [82,83] and random crystal field [84].  $S - 2$  Ising model on the Bethe lattice is the example of the  $S - 2$  Ising model with different geometry [85,86].

$S - 5/2$  Ising model has many experimental realizations as mentioned in [87]. This model has been solved within the EFT [88]. Also  $S - 5/2$  Ising model with transverse field [89], and quenched site dilution [90] problems were solved with EFT. Some other methods exist such as mean field renormalization group technique for the  $S - 5/2$  Ising model with random transverse field [91].

As seen from this short literature summary, many attempts have been made for the thermodynamical properties of the Spin- $S$  model. But there is less attention paid on the hysteresis behaviors. The aim of this work is to determine the hysteresis properties of the Spin- $S$  BC model and to obtain some general results especially about the multiple hysteresis behaviors. EFT for higher spin Ising model has been used in order to investigate hysteresis behaviors of the spin- $S$  BC model. First attempts of the constructing formulation can be found in Ref. [92] and decoupling approximation has been constructed in [93]. The most advanced version of the formulation can be found in a review article [94].

Very recently, it has been shown by the author that, crystal field diluted  $S - 1$  BC model could exhibit double and triple hysteresis behaviors at large negative values of the crystal field and the physical mechanisms behind these behaviors have been explained [95]. Also it has been demonstrated that isotropic Heisenberg model could not exhibit these types of behaviors [96]. The aim of the paper is obtain general results about the multiple hysteresis behaviors of the higher spin valued systems. For this aim, the paper is organized as follows: In Sec. 3 we briefly present the model and formulation. The results and discussions are presented in Sec. 4, and finally Sec. 5 contains our conclusions.

### 3 Model and Formulation

The Hamiltonian of the spin- $S$  BC model with uniform longitudinal magnetic field is given by

$$\mathcal{H} = -J \sum_{\langle i,j \rangle} s_i s_j - D \sum_i s_i^2 - H \sum_i s_i, \quad (1)$$

where  $s_i$  is the  $z$  component of the spin operator and it takes number of  $2S + 1$  different values such as  $s_i = -S, -S + 1, \dots, S - 1, S$ ,  $J > 0$  is the ferromagnetic exchange interaction between the nearest neighbor spins,  $D$  is the crystal field (single ion anisotropy),  $H$  is the external longitudinal magnetic field. The first summation in Eq. (1) is over the nearest-neighbor pairs of spins and the other summations are over all the lattice sites.

We can construct the EFT equations by starting with generalized Callen-Suzuki [97] identities, which are generalized versions of the identities for the  $S - 1/2$  system [98,99] and given as

$$\langle s_0^i \rangle = \left\langle \frac{Tr_0 s_0^i \exp(-\beta \mathcal{H}_0)}{Tr_0 \exp(-\beta \mathcal{H}_0)} \right\rangle, \quad (2)$$

where,  $i = 1, 2, \dots, 2S$  for the spin- $S$  Ising system and  $Tr_0$  is the partial trace over the site 0. Here,  $\mathcal{H}_0$  denotes to the all interactions of the spin that belongs to the site 0 and it has two parts as

spin-spin interactions (denoted as  $E_0$ ) and interactions with the fields (crystal field and magnetic field). From the Hamiltonian of the system represented by Eq. (1),  $\mathcal{H}_0$  is given by

$$\mathcal{H}_0 = s_0 (E_0 + H) + s_0^2 D, \quad E_0 = \sum_{\delta=1}^z s_\delta, \quad (3)$$

where  $z$  is the number of nearest neighbor interactions i.e. coordination number and  $s_\delta$  is the nearest neighbor of the spin located at site 0. Inserting Eq. (3) into Eq. (2) and performing partial trace operations produces the equations in closed form as,

$$\langle s_0^i \rangle = \langle F_i(E_0, H, D) \rangle. \quad (4)$$

By using differential operator technique [100], this equation can be written in the form

$$\langle s_0^i \rangle = \langle \exp(E_0 \nabla) \rangle F_i(x, H, D), \quad (5)$$

where  $\nabla$  is the differential operator with respect to  $x$  and the effect of the exponential differential operator on an arbitrary function  $F(x)$  is given by

$$\exp(a \nabla) F(x) = F(x + a), \quad (6)$$

where  $a$  is any constant. In this step, the exponential operator has  $s_\delta$  terms in the exponent and for the aim of constructing the equations, we have to obtain polynomial forms of the equations in  $s_\delta$ . In order to get polynomial form of Eq. (5), van der Waerden identities are often used:

$$\exp(as_k) = \sum_{i=0}^{2S} A_i(a) s_k^i. \quad (7)$$

The unknown coefficients  $A_i(a)$  can be obtained via the solutions of the  $2S + 1$  equations. These equations can be obtained by writing  $2S + 1$  possible values of the  $s_k = -S, -S + 1, \dots, S - 1, S$  in Eq. (7). By this way the nonlinear equation system which includes number of  $2S + 1$  equations for the spin- $S$  BC model can be obtained by Eq. (5) and solved numerically. But in order to avoid mathematical difficulties let us use approximated van der Waerden identities which were proposed for the higher spin problems [101] and it is given as

$$\exp(as_k) = \cosh(a\eta) + \frac{s_k}{\eta} \sinh(a\eta), \quad (8)$$

where  $\eta^2 = \langle s_k^2 \rangle$ . Note that this is the first approximation made in the formulation, but as discussed in [101] it produces accurate enough results in comparison with those obtained using the exact van der Waerden identity. Since this approximation equates  $s_k^{2n}$  to  $\langle s_k^2 \rangle^n$  and  $s_k^{2n+1}$  to  $s_k \langle s_k^2 \rangle^n$ , the number of  $2S + 1$  equations in Eq. (5) reduces to two. By using Eq. (8) these two equations can be written as

$$m = \langle s_0 \rangle = \left\langle \prod_{k=1}^z \left[ \cosh(J\eta \nabla) + \frac{s_k}{\eta} \sinh(J\eta \nabla) \right] \right\rangle F_1(x, H, D), \quad (9)$$

$$\eta^2 = \langle s_0^2 \rangle = \left\langle \prod_{k=1}^z \left[ \cosh(J\eta \nabla) + \frac{s_k}{\eta} \sinh(J\eta \nabla) \right] \right\rangle F_2(x, H, D). \quad (10)$$

Decoupling the terms  $s_k$  and  $s_k^2$  in the expanded form of Eqs. (9) and (10) and using the translationally invariance property of the lattice we arrive the equations:

$$m = \left[ \cosh(J\eta \nabla) + \frac{m}{\eta} \sinh(J\eta \nabla) \right]^z F_1(x, H, D), \quad (11)$$

$$\eta^2 = \left[ \cosh(J\eta \nabla) + \frac{m}{\eta} \sinh(J\eta \nabla) \right]^z F_2(x, H, D). \quad (12)$$

The explicit forms of the functions in Eqs. (11) and (12) can be obtained by performing partial trace operations in Eq. (2) for arbitrary  $S$  and they are given as

$$F_1(x, H, D) = \frac{\sum_{k=-S}^S k \exp(\beta D k^2) \sinh[\beta k(x + H)]}{\sum_{k=-S}^S \exp(\beta D k^2) \cosh[\beta k(x + H)]}, \quad (13)$$

$$F_2(x, H, D) = \frac{\sum_{k=-S}^S k^2 \exp(\beta D k^2) \cosh[\beta k(x + H)]}{\sum_{k=-S}^S \exp(\beta D k^2) \cosh[\beta k(x + H)]}. \quad (14)$$

By expanding Eqs. (11) and (12) with the help of Binomial expansion and applying Eq. (6) we get the equations as

$$m = \sum_{n=0}^z \binom{z}{n} \frac{m^n}{\eta^n} A_n^{(z)}, \quad (15)$$

$$\eta^2 = \sum_{n=0}^z \binom{z}{n} \frac{m^n}{\eta^n} B_n^{(z)}, \quad (16)$$

and the coefficients are given by

$$A_n^{(z)} = \frac{1}{2^z} \sum_{p=0}^{z-n} \sum_{q=0}^n \binom{z-n}{p} \binom{n}{q} (-1)^q F_1[\eta J(z - 2p - 2q)], \quad (17)$$

$$B_n^{(z)} = \frac{1}{2^z} \sum_{p=0}^{z-n} \sum_{q=0}^n \binom{z-n}{p} \binom{n}{q} (-1)^q F_2[\eta J(z - 2p - 2q)]. \quad (18)$$

By solving the system of nonlinear equations given by Eqs. (15) and (16) with the coefficients given by Eqs. (17) and (18) we get EFT - DA results for the spin- $S$  BC model. Linearization of Eqs. (15) and (16) in  $m$  will yield equation system for the second order critical temperature. Detailed investigation of the formulation used here can be found in review article [94].

## 4 Results and Discussion

For the numerical calculations, following scaled (dimensionless) quantities have been used

$$d = D/J, t = k_B T/J, h = H/J. \quad (19)$$

The hysteresis loops can be obtained for a given parameter set  $(d, t)$  by calculating the  $m$  according to the procedure given above, and by sweeping the longitudinal magnetic field from  $-h_0$  to  $h_0$  and then in reverse direction (i.e.  $h_0 \rightarrow -h_0$ ). We study on simple cubic lattice (i.e.  $z = 6$ ) within this work.

### 4.1 Phase diagrams

The phase diagrams of the spin- $S$  BC model in  $(d - t)$  plane can be seen in Figs. 1 (a) for integer  $S$  and (b) for half integer  $S$ . Indeed these diagrams have already been obtained in the literature with several methods. The phase diagrams for the  $S = 3/2$  BC model were obtained within thermodynamically self-consistent Ornstein-Zernike approximation [24], MC [25], EFT based on differential operator technique [19], EFT based on probability distribution technique [21] and pair

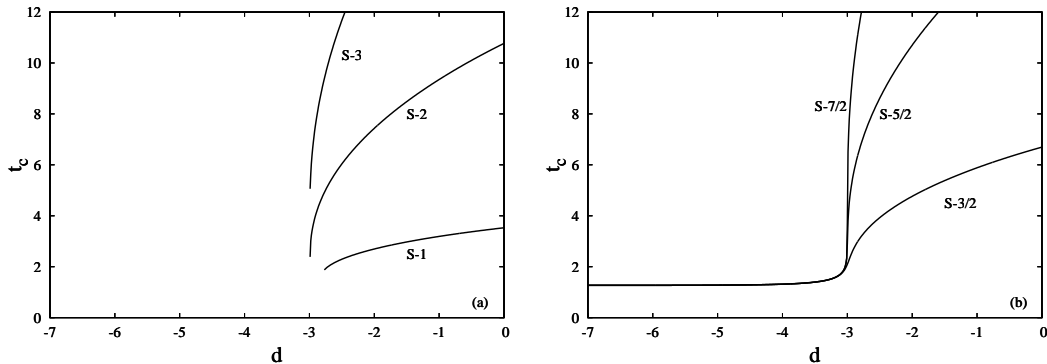


Figure 1: Variation of the critical temperature of the spin- $S$  BC model with crystal field. Fig. 1 (a) contains integer spins while (b) contains half integer spin models.

approximation [23]. The phase diagrams for the  $S - 2$  BC model obtained within MFA [83], EFT [71, 73, 76] and also for the  $S - 5/2$  BC model within EFT [88].

The main qualitative difference between the phase diagrams of integer (Fig. 1 (a)) and half integer (Fig. 1 (b)) spin model is seen for the large negative values of the crystal field. Integer spin models have non magnetic ground state, while half integer spin models have magnetic ground state for the large negative values of  $d$ . This is because of the fact that, for the large negative values of the crystal field, only the minimum value of the  $s_i$  makes the expectation value of the Hamiltonian given in Eq. (1) minimum. This minimum value is  $s = 0$  for the integer  $S$ , and  $s = \pm 1/2$  for half integer  $S$ . This means that for a ground state, rising  $d$  starting from  $d \rightarrow -\infty$  changes ground state from  $s = 0$  to  $s = S$  and  $s = 1/2$  to  $s = S$  for integer spin and half integer spin- $S$  BC model, respectively. These facts have been obtained by MFA [6], EFT [11, 47], pair approximation [23], pair approximation and MC [15]. It has been demonstrated in ground state that, for  $S - 3/2$  and  $S - 5/2$  BC models this transition occurs at  $D/J = -z/2$  where  $z$  is the coordination number [19, 88].

Another qualitative difference between the phase diagrams of integer (Fig. 1 (a)) and half integer (Fig. 1 (b)) spin model is tricritical point. As seen in Fig. 1 (a) and (b), integer spin model has tricritical point while half integer spin model has not.

Note that, in Fig. 1 (b) the phase diagram that lie along the large negative values of crystal field has temperature value  $t_c = 1.268$  which is just the critical temperature of the spin-1/2 model on simple cubic lattice.

## 4.2 Hysteresis behaviors

As demonstrated in Ref. [95],  $S - 1$  BC model has double hysteresis behavior for low temperature and large negative values of crystal field. This is due to the fact that, all spins of the system is in the state  $s = 0$  for low temperature and large negative values of crystal field. Magnetic field can induce transitions from this state to  $s = 1$  and  $s = -1$  states. In general, as seen in Fig. 1, Spin- $S$  BC model has ground state  $s = 0$  for integer  $S$  and  $s = 1/2$  for half integer  $S$  for large negative values of the crystal field. Then it is reasonable to think of that, the magnetic field can induce transition from  $s = 0$  to the state  $s = 1$  and further increasing field can induce transition from this state to  $s = 2$  and so on. In a similar manner, for a half integer  $S$ , rising longitudinal magnetic field induce a transition from  $s = 1/2$  to the state  $s = 3/2$ , if the magnetic field increases further this can cause transition to  $s = 5/2$  and so on. This plateau behavior of the magnetization has been demonstrated for antiferromagnetic  $S - 3/2$  and  $S - 2$  systems [30] and for  $S - 1$ ,  $S - 3/2$  and  $S - 5/2$  models on Bethe lattice [36]. If this behavior is history dependent, then this means that the model could show multiple hysteresis behavior.

In order to visualize these situations we depict some hysteresis loops of  $S - 2$  and  $S - 5/2$  BC models for selected values of Hamiltonian parameters and the temperature in Fig. 2. Indeed spin- $S$  BC model has hysteresis with  $2S$ -windows as seen in Figs. 2 (a) and (b), for large negative values

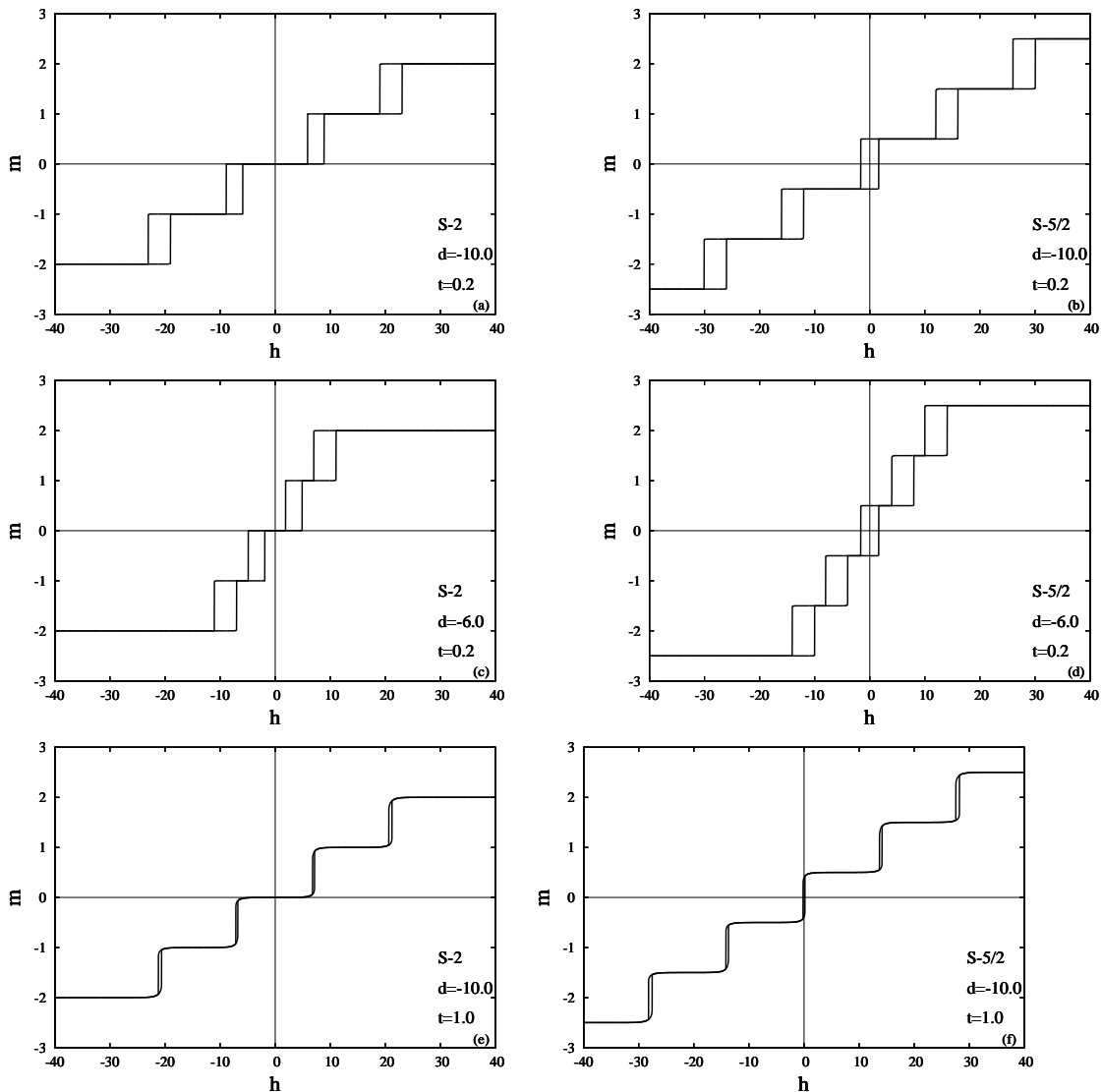


Figure 2: Hysteresis loops of  $S - 2$  and  $S - 5/2$  BC models for various values of  $d$  and  $t$ .

of  $d$  and low temperature. The difference between the half integer and integer  $S$  model is that, the hysteresis loop of the half integer model has central window (which is symmetric about the origin) while the hysteresis loop of the integer  $S$  model has not central loop (compare Figs. 2 (a) and (b)). This is due to the fact that, half integer model has ordered phase in large negative values of crystal field and low temperature, while integer spin model has not. We can conclude by comparing Figs. 2 (a) and (c), (b) and (d) with each other that, rising crystal field in negative direction causes the windows to be apart. Besides, the effect of the rising temperature can be seen by comparing Figs. 2 (a) and (e), (b) and (f). Rising temperature causes a shrink of the windows.

Interestingly, the hysteresis loop of spin- $S$  and spin- $(S+1)$  coincides, the only difference of latter hysteresis loop from the former loop is the outer windows (which are windows that appear in large negative and large positive values of the magnetic field). This can be seen in Fig. 3. Note that this nested structure of hysteresis loops of the successive Spin- $S$  BC model is independent of Hamiltonian parameters and the temperature (compare Figs. 3 (a) and (c), (b) and (d)). This structure can be interpreted as follows: transition from  $s = n$  to  $s = n + 1$  state requires the same amount of energy (which is supplied by the longitudinal magnetic field to the system in the case of hysteresis), regardless of the spin magnitude of the model. In other words the energy difference between  $s = n$  and  $s = n + 1$  states is the same for all values of  $S$ .

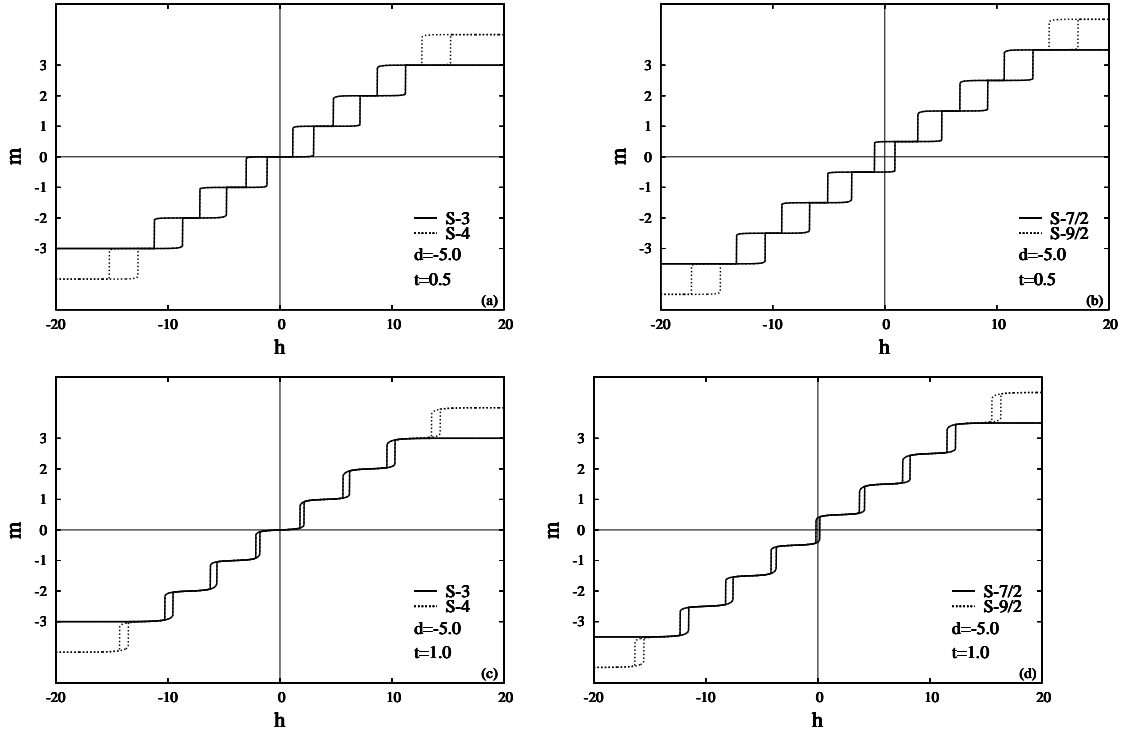


Figure 3: Hysteresis loops of the S-3, S-4 and S-7/2, S-9/2 BC models for selected values of  $d = -5.0$  and  $t = 0.5, 1.0$ .

Rising temperature causes shrink of the windows, as mentioned above. This shrinking behavior can be seen most dominantly on the closest windows to the center of the hysteresis loop, as temperature rises. This fact can be seen by comparing the central window of the hysteresis loops given in Figs. 2 (b) and (f) or 3 (b) and (d). The central window almost disappears, while the other windows survive. This shrinking process continues with disappearing of windows starting from the closest ones to the center of the loop, with rising temperature. While the temperature rises, the number of windows of the hysteresis loops of the integer spin- $S$  BC model changes as  $2S \rightarrow 2S - 2 \rightarrow \dots \rightarrow 2 \rightarrow 0$ . Similar sequence is valid for the half integer spin- $S$  BC model as  $2S \rightarrow 2S - 1 \rightarrow 2S - 3 \rightarrow \dots \rightarrow 2 \rightarrow 0$ . Hysteresis loop that has 0 number of windows means that, there is no history dependent variation of the order parameter on the longitudinal magnetic field. Note also that, all loops in given sequences are the loops of the paramagnetic phase except  $2S$  windows loop for the half integer spin- $S$  BC model. The transition of this loop to the  $2S - 1$  windowed loop occurs at the critical temperature of the spin- $S$  BC model, which is independent of the magnitude of the spin,  $t_c = 1.268$ .

Let the temperatures  $\tau_n^{i(S)}$  and  $\tau_n^{h(S)}$  be the temperatures of transition from the  $(n+2)$ -windows loop to the  $n$ -windows loop of the spin- $S$  BC model with integer and half integer  $S$ , respectively for large negative valued  $d$ . As seen in Fig. 3, rising temperature could not change the nested situation of the hysteresis loops of the spin- $S$  and spin- $(S+1)$  model. This means that, when the hysteresis loop of the spin- $(S+1)$  model passes to the  $(n+2)$ -windows structure from the  $n$ -windows structure, spin- $S$  model passes to the  $n$ -windows structure from the  $(n-2)$ -windows structure. In other words, for the transition temperatures for large negative values of the  $d$ , following equalities hold,

$$\begin{aligned}\tau_n^{i(S)} &= \tau_{n+2}^{i(S+1)}, n = 0, 2, \dots, 2S - 2 \\ \tau_n^{h(S)} &= \tau_{n+2}^{h(S+1)}, n = 0, 2, \dots, 2S - 3\end{aligned}$$

The variation of both  $\tau_n^{i(S)}$  and  $\tau_n^{h(S)}$  (as well as  $\tau_{n+1}^{i(S)} - \tau_n^{i(S)}$ ,  $\tau_{n+1}^{h(S)} - \tau_n^{h(S)}$ ) with  $n$  can be seen in Fig. 4 for  $S - 9$  and  $S - 19/2$  BC models. As seen in Fig. 4 (a), both of the transition

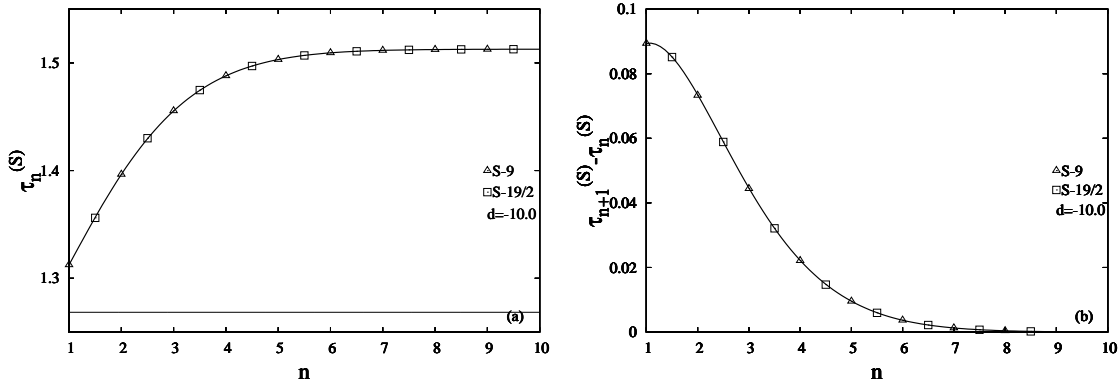


Figure 4: The variation of (a)  $\tau_n^{i(S)}$  and  $\tau_n^{h(S)}$  and (b)  $\tau_{n+1}^{i(S)} - \tau_n^{i(S)}$  and  $\tau_{n+1}^{h(S)} - \tau_n^{h(S)}$ , for  $S = 9$  (triangulars) and  $S = 19/2$  (squares) BC models. Lines are only guide for eye. Thin horizontal line represents the critical temperature of the half integer model for  $d = -10.0$ .

temperatures of integer and half integer spin model lie on the same curve. Besides, the difference between the temperatures of successive  $n$  values decreases, as seen in Fig. 4 (b). This means as  $S$  rising for spin- $S$  BC model, transitions between the higher  $n$ -windows loops could not be detected due to the low temperature differences.

## 5 Conclusion

Hysteresis characteristics of the general Spin- $S$  ( $S > 1$ ) Blume-Capel model have been studied within the effective field approximation. This work can be considered as the generalization of Ref. [95]. In that work it has been demonstrated that, S-1 BC model has double hysteresis behavior for large negative values of the crystal field and low temperature. In general, spin- $S$  BC model has  $2S$ -windowed hysteresis loop in the same region. The multiple hysteresis behavior is mostly attributed to different exchange interactions on some nanomaterials, such as nanowires. In this work simple physical mechanisms give rise to born of multiple hysteresis behavior given. Also the evolution of these multiple hysteresis loops with rising temperature and crystal field have been given and discussed. Besides, some interesting results have been obtained such as nested characteristics of the hysteresis loops of successive spin- $S$  Blume-Capel model.

In Ref. [96] it has been demonstrated that, the isotropic Heisenberg model could not exhibit multiple hysteresis behavior. Also crystal field dilution can induce transition from 2 window hysteresis loop to the 3 window loop in the S-1 Ising model. These results need to generalize and these generalizations will be our next works. We hope that the results obtained in this work may be beneficial form both theoretical and experimental points of view.

## References

- [1] J. P. Costes, A. Dupuis, J. P. Laurent, Eur. J. Inorg. Chem 1543-1546 (1998)
- [2] R. Sessoli, H. L. Tsai, A. R. Schake et al, J. Am. Chem. Soc., 115 (1993) 1804
- [3] E. Manuel, M. Evangelisti, M. Affronte et al, Phys. Rev. B 73 (2006) 172406
- [4] M. Blume, Physical Review 141 (1966) 517.
- [5] H. W. Capel, Physica 32 (1966) 966.
- [6] J.A. Plascak, J. G. Moreira, F.C. saBarreto, Phy. Lett. A 173 (1993) 360
- [7] J. W. Tucker, Journal of Magnetism and Magnetic Materials 71 (1987) 27
- [8] T. Iwashita, R. Satou, T. Imada, T. Idogaki Physica B 284-288 (2000) 1203
- [9] T. Kaneyoshi, M. Jascur, I. P. Fittipaldi Physical Review B 48 (1993) 250
- [10] A. Ainane, M. Saber Journal of Magnetism and Magnetic Materials 162 (1996) 230
- [11] T. Kaneyoshi, A. Benyoussef phys. stat. sol. (b) 178 (1993) 233
- [12] J. W. Tucker, M. Saber, L. Peliti Physica A 206 (1994) 497
- [13] T. Kaneyoshi Physica A 222 (1994) 450
- [14] D. P. Lara, J. A. Plascak Physica A 260 (1998) 443
- [15] D. P. Lara, J. A. Plascak, S. J. Ferreira et al Journal of Magnetism and Magnetic Materials 177-181 (1998) 163
- [16] A. H. Cooke, D. M. Martin, and M. R. Wells, J. Phys. Paris, Colloq. 32, C1-488 1971.
- [17] A. H. Cooke, D. M. Martin, and M. R. Wells, Solid State Commun. 9, 519 1971 .
- [18] S. Krinsky and D. Mukamel, Phys. Rev. B 11, 399 1975.
- [19] T. Kaneyoshi, M. Jascur Physica B 179 (1992) 317
- [20] T. Kaneyoshi, M. Jascur Physical Review B 46 (1992) 3374
- [21] L. Peliti, M. Saber phys. stat. sol. (b) 195 (1996) 537
- [22] W. Jiang, G. Z. Wei, Z. H. Xin phys. stat. sol. (b) 219 (2000) 157
- [23] V. Ilkovic Physica A 234 (1996) 545
- [24] S. Grollau Physical Review E 65 (2002) 056130
- [25] J. C. Xavier, F. C. Alcaraz, D. P. Lara et. all. Physical Review B 57 (1998) 11575
- [26] N. Tsushima, Y. Honda, T. Horiguchi Journal of the Physical Society of Japan 66 (1997) 3053
- [27] N. Tsushima, T. Horiguchi Journal of the Physical Society of Japan 67 (1998) 1574
- [28] A. Bakchich, S. Bekhechia, A. Benyoussef Physica A 210 (1994) 415
- [29] M. Keskin, M.A. Pinar, A. Erdinc et. all. Physics Letters A 353 (2006) 116
- [30] E. Aydiner, C. Akyuz, M. Gonulol phys. stat. sol. (b) 243 (2006) 2901
- [31] S. Bekhechi, A. Benyoussef, Physical Review B 56 (1997) 13954.
- [32] O. Ozsoy, M. Keskin Physica A 319 (2003) 404

- [33] O. Canko, M. Keskin *Physics Letters A* 320 (2003) 22
- [34] O. Baran, R. Levitskii *Physica B* 408 (2013) 88
- [35] E. Albayrak, M. Keskin *Journal of Magnetism and Magnetic Materials* 218 (2000) 121
- [36] C. Ekiz, H. Yaraneri *Journal of Magnetism and Magnetic Materials* 318 (2007) 49
- [37] E. Albayrak *Journal of Magnetism and Magnetic Materials* 232 (2011) 2846
- [38] N. Tahiri, H. Ez-Zahraouy, A. Benyoussef, *J Supercond Nov Magn* 26 (2013) 3143
- [39] N. Tahiri, H. Ez-Zahraouy, A. Benyoussef, *Physica A* 388 (1987) 3426
- [40] Y. Kocakaplan, M. Keskin, *Journal of Applied Physics* 116 (2014) 093904
- [41] Y. Kocakaplan, M. Ertas, *Journal of Experimental and Theoretical Physics* 121 (2015) 606
- [42] A. Bakchich, M. El Bouziani, *Physical Review B* 63 (2001) 064408.
- [43] O. Baran, R. Levitskii, *Journal of Magnetism and Magnetic Materials* 324 (2012) 3778.
- [44] W. Jiang, G. Wei, Z. Xin, *Journal of Magnetism and Magnetic Materials* 217 (2000) 225.
- [45] Y. Liang, G. Wei, Q. Zhang et al, *Journal of Magnetism and Magnetic Materials* 284 (2004) 47.
- [46] W. Jiang, Z. Lu, G. Wei et al *Communications in Theoretical Physics* 38 (2002) 227.
- [47] G. Wei, H. Miao, J. Liu et al, *Journal of Magnetism and Magnetic Materials* 315 (2007) 71.
- [48] W. Jiang, G. Wei, *Physica A* 284 (2000) 215.
- [49] W. J. Song, C. Z. Yang, *Solid State Communications* 91 (1994) 145.
- [50] W. Jiang, G. Wei, Z. Xin *phys. stat. sol. (b)* 218 (2000) 553.
- [51] W. Jiang, L. Guo, G. Wei et al *Physica B* 307 (2001) 15.
- [52] W. Jiang, G. Wei, A. Duc et al, *Physica A* 313 (2002) 503.
- [53] W. Jiang, G. Wei, Q. Zhang, *Physica A* 329 (2003) 161.
- [54] Y. Liang, G. Wei, H. Zhang et al *Communications in Theoretical Physics* 42 (2004) 467.
- [55] Y. Liang, G. Wei, Q. Zhang, *Journal of Magnetism and Magnetic Materials* 265 (2003) 305.
- [56] Y. Liang, G. Wei, Q. Zhang, *Journal of Magnetism and Magnetic Materials* 267 (2003) 275.
- [57] M. Jascur, T. Kaneyoshi, *Physica A* 195 (1993) 497.
- [58] Y. Liang, G. Wei, G. Song, *phys. stat. sol. (b)* 241 (2004) 3636.
- [59] A. Yigit, E. Albayrak, *Chinese Physics B* 22 (2013) 100508.
- [60] M. Bouziani, A. Gaye, *Physica A* 392 (2013) 2643.
- [61] L. Bahmad, A. Benyoussef, A. El Kenz, *Journal of Magnetism and Magnetic Materials* 320 (2008) 397.
- [62] A. Ainane, A. El-Atri, M. Kerouad et al *Journal of Magnetism and Magnetic Materials* 146 (1995) 283.
- [63] A. El-Atri, A. Ainane, M. Saber, *phys. stat. sol. (b)* 193 (1996) 477.
- [64] M. Kerouad, A. El-Atri, A. Ainane et al. *phys. stat. sol. (b)* 195 (1996) 519.

- [65] L. Y. Xing, S. L. Yan, *Journal of Magnetism and Magnetic Materials* 324 (2012) 3641.
- [66] T. Kaneyoshi, M. Jascur, *phys. stat. sol. (b)* 173 (1992) K37.
- [67] A. Bakkali, M. Kerouad, M. Saber, *phys. stat. sol. (b)* 186 (1994) 505.
- [68] C. Mathoniere, C.J. Muttall, S.G. Carling, P. Day, *Inorganic Chemistry* 35 (1996) 1201.
- [69] U. Koebler, J. Englich, O. Hupe, and J. Hesse, *Physica B* 339 (2003) 156.
- [70] A. S. Freitas, Douglas F. de Albuquerque, I. P. Fittipaldi, and N. O. Moreno *Journal of Applied Physics* 113 (2013) 093903
- [71] W. Jiang, G. Wei, Z. Xin *Journal of Magnetism and Magnetic Materials* 220 (2000) 96.
- [72] G. Wei, H. Miao, J. Liu et al *Journal of Magnetism and Magnetic Materials* 320 (2008) 1151.
- [73] W. Jiang, G. Wei, Z. Xin, *phys. stat. sol. (b)* 225 (2001) 215.
- [74] J. Wei, G. Wei, A. Du et al *Chinese Physics* 11 (2002) 823.
- [75] W. Jiang, G. Wei, Z. Xin, *phys. stat. sol. (b)* 221 (2000) 759.
- [76] Y. Liang, G. Wei, Q. Zhang et al, *Chinese Physics Letters* 21 (2004) 378.
- [77] Q. Liang, G. Wei, L. Song et al, *Communications in Theoretical Physics* 42 (2004) 623.
- [78] A. Yigit, E. Albayrak, *Chinese Physics B* 21 (2012) 110503.
- [79] M. saber, J. W. Tucker, *Physica A* 217 (1995) 407.
- [80] H. El Mir, M. Saber, J. W. Tucker, *Journal of Magnetism and Magnetic Materials* 138 (1994) 76.
- [81] W. Jiang, A. Guo, X. Lin et al *Communications in Theoretical Physics* 46 (2006) 1105.
- [82] J. Zhao, G. Wei, X. Xu, *Communications in Theoretical Physics* 45 (2006) 749.
- [83] J. Zhao, X. Xu, G. Wei, *Communications in Theoretical Physics* 52 (2009) 163.
- [84] L. Bahmad, A. Benyoussef, A. El Kenz, *Physical Review B* 76 (2007) 094412.
- [85] E. Albayrak, S. Akkaya, S. Yilmaz, *International Journal of Modern Physics B* 22 (2008) 4877.
- [86] E. Albayrak, S. Akkaya, S. Yilmaz, *International Journal of Modern Physics B* 24 (2012) 4189.
- [87] M. Ertas, M. Keskin, B. Deviren, *Journal of Magnetism and Magnetic Materials* 324 (2012) 1503.
- [88] T. Kaneyoshi, M. Jascur, *phys. stat. sol. (b)* 175 (1993) 225.
- [89] M. Saber, J. W. Tucker, *phys. stat. sol. (b)* 189 (1995) 229.
- [90] M. Kerouad, M. Saber, J. W. Tucker, *Physica A* 210 (1994) 424.
- [91] W. J. Song, C. Z. Yang *Solid State Communications* 92 (1994) 361.
- [92] T. Kaneyoshi, J. W. Tucker, M. Jascur, *Physica A* 186 (1992) 495.
- [93] T. Kaneyoshi, *Physica A* 286 (2000) 518.
- [94] J. Strecka, M. Jascur, *acta physica slovacca* 65 (2015) 235.
- [95] Ü. Akıncı, *Physics Letters A* 380 (2016) 1352
- [96] Ü. Akıncı, *Journal of Magnetism and Magnetic Materials* 397 (2016) 247

- [97] T. Balcerzak, *J. Magn. Magn. Mater.* 246 (2002) 213.
- [98] H.B. Callen, *Phys. Lett.* 4 (1963) 161.
- [99] M. Suzuki, *Phys. Lett.* 19 (1965) 267.
- [100] R. Honmura, T. Kaneyoshi, *J. Phys. C: Solid State Phys.* 12 (1979) 3979.
- [101] T. Kaneyoshi, J. Tucker, M. Jascur, *Physica A* 176, 495 (1992).